Mechanics Of Soft Materials (2020) 2:7
https://doi.org/10.1007/s42558-020-00022-7

ORIGINAL PAPER

Residual stresses reduce pulse wave velocity in arteries

P. Mythravaruni[1,2] · K. Y. Volokh[1]

Received: 3 January 2020 / Accepted: 29 April 2020
© Springer Nature Switzerland AG 2020

Abstract
In this note, we develop simple analytical formulas to estimate the effect of residual stresses on the pulse wave velocity in blood vessels. We combine these formulas with three constitutive models of the arterial wall. Particularly, we consider the Fung model and two models accounting for the dispersion of collagen fibers via 8 and 16 structure tensors accordingly. The residual stresses come into play with a description of the initial kinematics—the opening angle. Our numerical examples reveal that residual stresses reduce the pulse wave velocity. The latter effect becomes especially pronounced at high values of blood pressure.

Keywords Residual stresses · Pulse wave velocity · Constitutive models

1 Introduction

Blood pressure is one of the significant health indicators. Many factors such as physical exercise, emotional, and physiological states affect blood pressure. Excessive fall and rise in blood pressure leads to accompanying disorders, hypotension and hypertension, respectively [1–3]. Conventionally, blood pressure is measured by releasing the external pressure that is imparted to the arm by an inflating cuff, which brings the blood flow to halt temporarily [4]. This cannot be used for continuous monitoring of blood pressure. Continuous monitoring is possible only through invasive procedures that rely on the measurements of intra-arterial pressure [5]. These techniques put patients at a disadvantage of exposure to risk of complications and, hence, call for intensive care [6]. Blood pressure measurement alone cannot provide any conclusive prediction of the health status of heart.

Pulse wave velocity (PWV) is described by the velocity with which the blood pressure pulse propagates in arteries. Pulse wave velocity measurement is suitable for continuous and noninvasive monitoring of blood pressure [7–10]. The Moens-Korteweg equation [11] was used together with Hughes equation [12] to correlate the blood pressure to the measured pulse wave velocity (PWV): $\mathrm{PWV} = \sqrt{Eh_0/(2\rho R_0)}$ and $E = E_0 \exp(\zeta p)$, where p is the blood pressure, E_0 is the elastic modulus at zero blood pressure, ζ is a material coefficient of artery, ρ is the blood mass density, and h_0 and R_0 are the initial wall thickness and radius of artery.

The Moens-Korteweg equation was developed based on the assumptions that the artery wall was thin and its thickness and radius were constant. In reality for human arteries, the thickness to radius ratio varies with blood pressure [13] and the thickness to radius ratio is much higher than the range which can be used for thin shell [14]. Recently, it was proposed [15], instead of the Moens-Korteweg equation, to use formula $\mathrm{PWV} = \sqrt{(s/\rho)dp/ds}$, where s is the inner cross-sectional area of the artery, together with Fung's hyperelastic constitutive model [16] for the arterial wall. This new formula is valid for arteries with thick walls and with thickness to radius ratio varying with blood pressure.

✉ P. Mythravaruni
varuni.mythra@gmail.com

[1] Faculty of Civil and Environmental Engineering, Technion – I.I.T., Haifa, Israel

[2] Present address: IIT Madras, Chennai, Tamil Nadu, India

Published online: 22 May 2020

In the present work, we make the next step and develop simple analytical formulas to estimate the effect of residual stresses—prestresses—on the pulse wave velocity in blood vessels. We combine these formulas with three constitutive models of the arterial wall. Particularly, we consider the Fung model and two models accounting for the dispersion of collagen fibers via 8 and 16 structure tensors accordingly. The residual stresses come into play with a description of the initial kinematics—the opening angle.

We note in passing that residual stresses can affect mechanical behavior of materials in various and unexpected ways. We refer to [20] and [21] for the effect of residual stresses on surface wave propagation and bifurcation in soft materials and structures accordingly.

2 Pulse wave velocity

We refer to [17] for the general theoretical background and notation.

With account of axial symmetry, nontrivial equilibrium equations for the arterial wall in cylindrical coordinates reduce to

$$r\frac{\partial \sigma_{rr}}{\partial r} = \lambda_\varphi \frac{\partial \psi}{\partial \lambda_\varphi} - \lambda_r \frac{\partial \psi}{\partial \lambda_r}, \tag{1}$$

where σ_{rr} is the principal Cauchy stress in the radial direction and $\psi(\lambda_r, \lambda_\varphi, \lambda_z)$ is the strain energy density depending on the principal stretches in directions of cylindrical coordinates r, φ, z.

With account of incompressibility, $\lambda_r\lambda_\varphi\lambda_z = 1$, we can introduce a reduced strain energy function

$$w(\lambda, \lambda_z) = \psi(\lambda_r, \lambda_\varphi, \lambda_z) = \psi(\lambda^{-1}\lambda_z^{-1}, \lambda, \lambda_z). \tag{2}$$

Then, we calculate

$$\begin{aligned}\frac{\partial w}{\partial \lambda} &= \frac{\partial \psi}{\partial \lambda_r}\frac{\partial \lambda_r}{\partial \lambda} + \frac{\partial \psi}{\partial \lambda_\varphi}\frac{\partial \lambda_\varphi}{\partial \lambda} + \frac{\partial \psi}{\partial \lambda_z}\frac{\partial \lambda_z}{\partial \lambda} \\ &= \frac{\partial \psi}{\partial \lambda_\varphi} - \frac{1}{\lambda^2\lambda_z}\frac{\partial \psi}{\partial \lambda_r},\end{aligned} \tag{3}$$

or

$$\lambda_\varphi \frac{\partial \psi}{\partial \lambda_\varphi} - \lambda_r \frac{\partial \psi}{\partial \lambda_r} = \lambda \frac{\partial w}{\partial \lambda}. \tag{4}$$

Now, Eq. 1 can be rewritten as follows

$$r\frac{\partial \lambda}{\partial r}\frac{\partial \sigma_{rr}}{\partial \lambda} = \lambda \frac{\partial w}{\partial \lambda}. \tag{5}$$

Further transformation of the equilibrium equation requires calculation of $\partial\lambda/\partial r$. For this purpose, we use the incompressibility condition in the form

$$\gamma\lambda_z(r^2 - a^2) = R^2 - A^2, \tag{6}$$

where $\gamma = 2\pi/(2\pi - \omega)$ and ω is the artery opening angle after the cut; r, a and R, A are the radial coordinate and internal radius of the artery in the current and referential configurations accordingly.

Consequently, we have

$$\lambda = \gamma r R^{-1} = \gamma r(\gamma\lambda_z(r^2 - a^2) + A^2)^{-1/2}, \tag{7}$$

and, by the direct calculation,

$$r\frac{\partial \lambda}{\partial r} = \lambda(1 - \lambda_z\gamma^{-1}\lambda^2). \tag{8}$$

Substitution of Eq. 8 in Eq. 5 yields

$$\frac{\partial \sigma_{rr}}{\partial \lambda} = \frac{1}{1 - \lambda_z\gamma^{-1}\lambda^2}\frac{\partial w}{\partial \lambda}. \tag{9}$$

Integrating Eq. 9 we get for the blood pressure on the arterial wall

$$p(\lambda_a) = \int_{\lambda_b(\lambda_a)}^{\lambda_a} \frac{w' d\lambda}{\lambda_z\gamma^{-1}\lambda^2 - 1}, \tag{10}$$

Table 1 Material constants for Fung's model [16]

c	c_1	c_2	c_3	c_4	c_5	c_6
26.95 kPa	0.0089	0.9925	0.418	0.0193	0.0749	0.0295

where $w' \equiv \partial w/\partial\lambda$; $\lambda_a = \gamma a/A$; $\lambda_b = \gamma b/B$; and

$$\lambda_b = \sqrt{\lambda_a^2 A^2 B^{-2} + (1 - A^2 B^{-2})\gamma\lambda_z^{-1}} \tag{11}$$

by virtue of the incompressibility condition.

According to Fung [13], the pulse wave velocity is calculated as follows

$$\mathrm{PWV} = \sqrt{\frac{s}{\rho}\frac{\partial p}{\partial s}}, \tag{12}$$

where $s = \pi a^2$ is the artery internal cross-section area and ρ is the blood mass density.

In terms of the boundary stretch λ_a, we can rewrite Eq. 12 as follows

$$\mathrm{PWV} = \sqrt{\frac{\lambda_a}{2\rho}\frac{\partial p}{\partial \lambda_a}}, \tag{13}$$

where the pressure derivative is calculated from Eq. 10 analytically

$$\frac{\partial p}{\partial \lambda_a} = \frac{w'(\lambda_a)}{\lambda_z\gamma^{-1}\lambda_a^2 - 1} - \frac{w'(\lambda_b)}{\lambda_z\gamma^{-1}\lambda_b^2 - 1}\frac{\lambda_a}{\lambda_b}\frac{A^2}{B^2}. \tag{14}$$

Thus, we finally have (compare also with [18])

$$\mathrm{PWV} = \sqrt{\frac{\lambda_a}{2\rho}\left\{\frac{w'(\lambda_a)}{\lambda_z\gamma^{-1}\lambda_a^2 - 1} - \frac{w'(\lambda_b)}{\lambda_z\gamma^{-1}\lambda_b^2 - 1}\frac{\lambda_a}{\lambda_b}\frac{A^2}{B^2}\right\}}. \tag{15}$$

3 Constitutive models of arterial wall

We consider the following three models of the arterial wall.

The Fung constitutive model [16] is defined by the following strain energy density function

$$\begin{aligned} w(\lambda, \lambda_z) = \frac{c}{2}\Bigg\{\exp\Bigg[&\frac{c_1}{4}\left(\lambda^{-2}\lambda_z^{-2} - 1\right)^2 + \frac{c_2}{4}\left(\lambda^2 - 1\right)^2 \\ &+ \frac{c_3}{4}\left(\lambda_z^2 - 1\right)^2 + \frac{c_4}{2}\left(\lambda^{-2}\lambda_z^{-2} - 1\right)\left(\lambda^2 - 1\right) \\ &+ \frac{c_5}{2}\left(\lambda^2 - 1\right)\left(\lambda_z^2 - 1\right) + \frac{c_6}{2}\left(\lambda^{-2}\lambda_z^{-2} - 1\right) \\ &\left(\lambda_z^2 - 1\right)\Bigg] - 1\Bigg\}, \end{aligned} \tag{16}$$

where material constants c and c_i, fitted in tests on rabbit carotid arteries, are given in Table 1.

Table 2 Material constants for model with 8 (left) and 16 (right) structure tensors [19]

c	k_1	k_2	c	k_1	k_2
5 kPa	2.04 kPa	1.58	5 kPa	2.23 kPa	1.63

Table 3 Material parameters for models with 8 (left) and 16 (right) structure tensors [19]

$\Phi^{(i)}$	$\Theta^{(i)}$	$\alpha^{(i)}$	$\Phi^{(i)}$	$\Theta^{(i)}$	$\alpha^{(i)}$
10°	90°	0.440527	10°	82.5°	0.211123
34°	90°	2.6916	34°	82.5°	1.28996
59°	90°	2.36997	59°	82.5°	1.13581
80°	90°	0.724365	80°	82.5°	0.347153
100°	90°	0.724365	100°	82.5°	0.347153
121°	90°	2.36997	121°	82.5°	1.13581
146°	90°	2.6916	146°	82.5°	1.28996
170°	90°	0.440527	170°	82.5°	0.211123
			10°	97.5°	0.211123
			34°	97.5°	1.28996
			59°	97.5°	1.13581
			80°	97.5°	0.347153
			100°	97.5°	0.347153
			121°	97.5°	1.13581
			146°	97.5°	1.28996
			170°	97.5°	0.211123

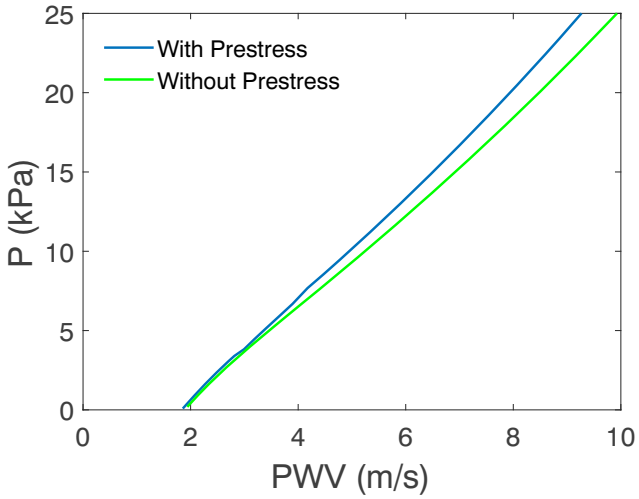

Fig. 1 Pressure versus pulse wave velocity with and without residual stress for Fung's model

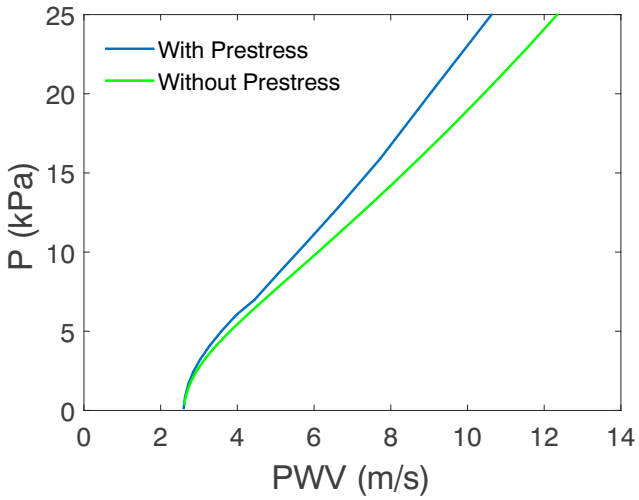

Fig. 2 Pressure versus pulse wave velocity with and without residual stress for the model with 8 structure tensors

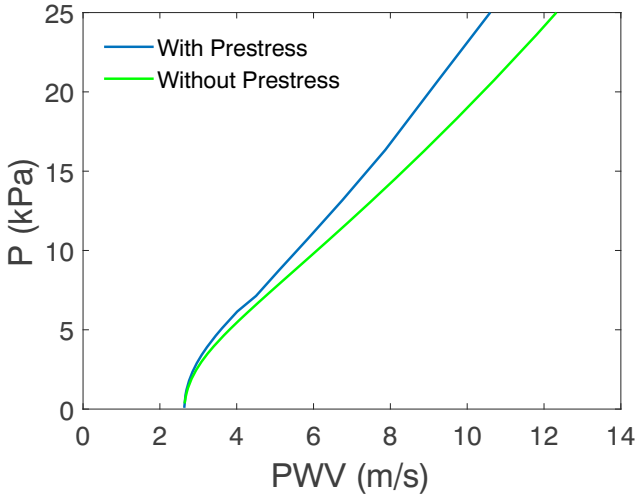

Fig. 3 Pressure versus pulse wave velocity with and without residual stress for the model with 16 structure tensors

Two constitutive models with fiber dispersion [19] include $N = 8$ and $N = 16$ structure tensors and the strain energy density function is defined as follows

$$\begin{aligned} w(\lambda, \lambda_z) = & \frac{c}{2}(\lambda\lambda_z^{-2} + \lambda^2 + \lambda_z^2 - 3) \\ & + \frac{k_1}{2k_2}\sum_{i=1}^{N}\alpha^{(i)}\{\exp[k_2((\lambda\cos\Phi^{(i)}\sin\Theta^{(i)})^2 \\ & + (\lambda_z\sin\Phi^{(i)}\sin\Theta^{(i)})^2 + (\lambda^{-1}\lambda_z^{-1}\cos\Theta^{(i)})^2 \\ & - 1)^2] - 1\}, \end{aligned} \tag{17}$$

where material constants c, k_1, k_2 and parameters $\alpha^{(i)}$, $\Phi^{(i)}$, $\Theta^{(i)}$, fitted in [19] to the experimental data on human arteries, are given in Tables 2 and 3 accordingly.

4 Results

We calculate the blood pressure and the pulse wave velocity from Eqs. 10 and 15 accordingly as functions of the current internal radius of the artery. This radius can be interpreted as a parameter, which is excluded from the pressure-velocity plots. Such plots are shown in Figs. 1, 2, and 3 for arterial models described above. These plots were generated for $\gamma = 1.8$ ($\omega = 160°$), $\lambda_z = 1$, $A = 1.43$ mm, and $B = 1.82$ mm with account of residual stresses and $\gamma = 1$ ($\omega = 0°$), $\lambda_z = 1$, $A = 0.71$ mm, and $B = 1.1$ mm without residual stresses. The blood mass density was $\rho = 1060\,\mathrm{kg/m^3}$.

All plots show monotonic decrease of the pulse wave velocity with the increase of residual stresses in the physiological range. The difference can reach 20% for high pressures.

5 Conclusion

In this note, we presented a simple analytical study of the effect of residual stresses—prestresses—on the pulse wave velocity of blood in arteries. We found that the residual stresses generally reduced the pulse wave velocity.

References

1. Lewington, S., Clarke, R., Qizilbash, N., Peto, R., Collins, R.: Prospective studies collaboration. Age-specific relevance of usual blood pressure to vascular mortality: a meta-analysis of individual data for one million adults in 61 prospective studies. Lancet. **360**, 1903–1913 (2002)
2. Mendez, A.S., Melgarejo, J.D., Mena, L.J., Chávez, C.A., González, A.C., Boggia, J., Terwilliger, J.D., Lee, J.H., Maestre, G.E.: Risk factors for orthostatic hypotension: differences between elderly men and women. Am J Hypertens. **31**, 797–803 (2018)
3. SPRINT Research Group, Wright, J.T.Jr., Williamson, J.D., Whelton, P.K., Snyder, J.K., Sink, K.M., Rocco, M.V., Reboussin, D.M., Rahman, M., Oparil, S., Lewis, C.E., Kimmel, P.L., Johnson, K.C., Goff, D.C.Jr., Fine, L.J., Cutler, J.A., Cushman, W.C., Cheung, A.K., Ambrosius, W.T.: A randomized trial of intensive versus standard blood-pressure control. N Eng J Med. **373**, 2103–2116 (2015)
4. McLaughlin, A.R.: A modified Erlanger sphygmomanometer. Science. **67**, 72–73 (1928)
5. Berkelmans, G.F.N., Kuipers, S., Westerhof, B.E., Spoelstrade Man, A.M.E., Smulders, Y.M.: Comparing volume-clamp method and intra-arterial blood pressure measurements in patients with atrial fibrillation admitted to the intensive or medium care unit. J. Clin. Monit Comput. **32**, 439–446 (2018)
6. Scheer, B., Perel, A., Pfeiffer, U.J.: Clinical review: complications and risk factors of peripheral arterial catheters used for haemodynamic monitoring in anaesthesia and intensive care medicine. Crit Care. **6**, 199–204 (2002)
7. Peter, L., Noury, N., Cerny, M.: A review of methods for non-invasive and continuous blood pressure monitoring: pulse transit time method is promising? IRBM. **35**, 271–282 (2014)
8. Sharma, M., Barbosa, K., Ho, V., Griggs, D., Ghirmai, T., Krishnana, S.K., Hsiai, T.K., Chiao, J.-C., Cao, H.: Cuff-less and continuous blood pressure monitoring: a methodological review. Technologies. **5**, 21 (2017)
9. Boutry, C.M., Nguyen, A., Lawal, Q.O., Chortos, A., Rondeau-Gagné, S., Bao, Z.: A sensitive and biodegradable pressure sensor array for cardiovascular monitoring. Adv Mater. **27**, 6954–6961 (2015)
10. Kastuura, T., Izumi, S., Yoshimoto, M., Kawaguchi, H., Yoshimoto, S., Sekitani, T.: IEEE Biomedical Circuits and Systems Conference (BioCAS) (Inst Electr Electron Eng, New York), abstr 7208 (2017)
11. Bramwell, J.C.: The velocity of the pulse wave in man. Proc. R. Soc. B. **93**, 298–306 (1922)
12. Hughes, D.J., Babbs, C.F., Geddes, L.A., Bourland, J.D.: Measurements of Young's modulus of elasticity of the canine aorta with ultrasound. Ultrason. Imaging. **1**, 356–367 (1979)
13. Fung, Y.C.: Biomechanics: Circulation. Springer, New-York (1997)
14. Timoshenko, S.: Theory of Plates and Shells. McGraw-Hill, London (1940)
15. Ma, Y., Choi, J., Hourlier-Fargette, A., Xue, Y., Chung, H.K., Lee, J.Y., Wang, X., Xie, Z., Kang, D., Wang, H., Han, S., Kang, S.K., Kang, Y., Yu, X., Slepian, M.J., Raj, M.S., Model, J.B., Feng, X., Ghaffari, R., Rogers, J.A., Huang, Y.: Relation between blood pressure and pulse wave velocity for human arteries. Proc. Natl. Acad. Sci. **115**, 11144–11149 (2018)
16. Fung, Y.C.: Biomechanics: Mechanical Properties of Living Tissues. Springer, New-York (1993)
17. Volokh, K.Y.: Mechanics of Soft Materials. Springer, Singapore (2019)
18. Fu, Y.B., Il'ichev, A.T.: Localized standing waves in a hyperelastic membrane tube and their stabilization by a mean flow. Math Mech. Solids. **20**, 1198–1214 (2015)
19. Volokh, K.Y.: On arterial fiber dispersion and auxetic effect. J Biomech. **61**, 123–130 (2017)
20. Nam, N.T., Merodio, J., Ogden, R.W., Vinh, P.C.: The effect of initial stress on the propagation of surface waves in a layered half-space. Int J Solids Struct. **88-89**, 88–100 (2016)
21. Dehghani, H., Desena-Galarza, D., Jha, N.K., Reinoso, J., Merodio, J.: Bifurcation and post-bifurcation of an inflated and extended residually-stressed circular cylindrical tube with application to aneurysms initiation and propagation in arterial wall tissue. Finite Elem Anal Design **161**, 51–60 (2019)

Publisher's note Springer Nature remains neutral with regard to jurisdictional claims in published maps and institutional affiliations.